

# Revealing the Nature of Strong Lensing System J1436+4943 with Only the MaNGA Data

**Zimen Wan**

High School affiliated to Renmin University, Beijing 100080, China

wanzimeng1012@163.com

**Abstract.** Strong gravitational lensing is a powerful tool for probing the mass content of the Universe. Both high-resolution imaging and spectroscopy observations are important for identifying and measuring the properties of the lensing object. The strong lensing system J1436+4943 was discovered in the SDSS-IV MaNGA survey and further observed with the FOCAS IFU spectrograph on the Subaru Telescope. We investigate whether comparable properties, e.g., the Einstein radius can be obtained using only MaNGA data cubes. The result shows that the general properties of the lens system can be recovered but the Einstein radius is different from the result with FOCAS IFU data by less than 25%. The MaNGA data cubes are helpful for fast analysis of large samples and to study the statistical properties of gravitational lensing systems.

**Keywords:** strong gravitational lensing, MaNGA spectroscopy.

## 1. Introduction

Gravitational lensing is a phenomenon that occurs when massive foreground objects, such as galaxies and galaxy clusters, warp the fabric of space itself [1] and thus bend the light path. Multiple light paths are allowed from the background source to the observer, so multiple images are formed. This phenomenon is useful in different fields. In microlensing, the multiple images cannot be resolved with current instruments. However, by observing the total magnification pattern due to the lens focusing over time, one can detect exoplanets in the lens system. In strong gravitational lensing, the multiple images can be resolved so the wealth of information contained in these images, e.g., their relative position, flux ratio, and arrival time, allows scientists to derive new statistical constraints on the dark matter mass function [2] and study the mass distribution of the lensing galaxy at the smallest angular scales [3].

To harness the power of gravitational lensing, we need a large sample of strong lensing systems. However, the low lensing probability makes it a challenge to find out the strong lensing systems among billions of galaxies. It is difficult to perform strong lens detection with the human eyes [4]. In 2002, the Cosmic Lens All Sky Survey (CLASS) [5] selected 22 multiply-imaged lens systems out of 16,503 northern hemisphere sources through visual inspection of each source along with the Caltech DIfference MAPping package (DIFMAP) [6] analyzing the modeling results of each source. To make sure the results are valid, the process was repeated several times by different people. Via visual inspection, the rare lens system can be found but the process is time-consuming. Apart from using images, spectroscopic detection is also a means of discovery. Spectroscopic detection can be used to isolate a lens system in a wide field by looking for pairs of objects with different redshifts in the same

line of sight. This method has proven itself with Sloan Lens ACS [7] and BOSS Emission-Line Lens Survey [8]. However, this method is technically expensive as an image-based lens search method and can only be carried out for a limited number of dedicated blank surveys [4]. With the construction and growth of sky surveys, the amount of detected data has increased rapidly. The previous way of searching for strong gravitational lensing systems became unfeasible for future large surveys. Therefore, automation became necessary. In recent years, machine learning has been widely used in many fields. The field of strong gravitational lensing also uses machine learning to search for strong gravitational lensing systems, such as the Manchester-SVM [9]. The Manchester-SVM is based on Support Vector Machine (SVM), which is a supervised machine learning method.

Among these surveys, Talbot et al. (2018) [10] introduce a spectroscopic identification of lensing objects (SILO) survey based on the MaNGA MPL-5 data. The principle of this SILO survey is to determine whether the system is a strong gravitational lens by searching and studying the background emission lines of the system. The first step to be performed is foreground galaxy subtraction, by utilizing a basis of seven principal component analysis (PCA) eigen-spectra to construct a best-fit model spectrum to the foreground galaxy, and then subtracting this continuum model from the data to obtain a spectrum for the background galaxy [10]. The next step is background emission-line detection, which detects all background emission-lines and grades the hits that contain the form of a  $[O_{II}]$  doublet, or multiple patterns of background emission-lines as good hits [10]. Since the MaNGA data are observed in multi-fibers, the candidate background emission lines can be spatially correlated to further confirm that the emission lines selected in the previous step are reliable [10]. If so, the Einstein radius of all candidate systems is calculated. The following step is source-plane inspection, which inspects each source plane that contains good hits, through manual inspection to check for spatial correlation in the emission-line features of good hits [10]. Finally, strong lensing candidates are selected by the factors, such as the number of good hits in each source plane, the location of imaging, etc. This survey selected 36 promising candidates. We analyze one of these candidates, the J1436+4943 system, which has been further observed with the FOCAS IFU spectrograph on the Subaru Telescope [1].

The J1436+4943 system is a strong gravitational lensing system in the SDSS-IV MaNGA survey database. Talbot et al. [10] first identified the J1436+4943 system as a potential multiple-imaging system. The foreground galaxy is at redshift  $z = 0.125$ . The background  $[O_{II}]$  emission from the background galaxy at redshift  $z = 1.231$  forms two separate arcs [1]. Figure 1 shows the MaNGA optical image of the J1436+4943 system observed in the sky. We use only the MaNGA data to derive the properties of the J1436+4943 system to test the accuracy and feasibility of using the MaNGA data to study strong gravitational lensing systems.

In this paper, Section 2 presents the MaNGA dataset. We introduce the spectral feature extraction procedures for the J1436+4943 system to extract the  $OII$  doublet narrow-band lensed image in Section 3. Section 4 shows the modeling methods, which are comprised of two algorithms, the Particle Swarm Optimization (PSO), and the Markov chain Monte Carlo algorithm (MCMC). The results of the modeling are also presented in Section 4. We summarize the work in Section 5. In Section 6, we draw the conclusion.

We adopt the cosmological parameters from Planck 2015 results [11].



**Figure 1.** The MaNGA optical image of the J1436+4943 system. The image represents a 30 arcsec by 30 arcsec region around the lensing galaxy. The object coordinates of is (RA, DEC) = (14h36m07.56s, +49d43m13.22s) (J2000).

## 2. Introduction of MaNGA Data

We use MaNGA data to study the J1436+4943 system. MaNGA is one of the surveys that make up SDSS-IV, the fourth phase of the Sloan Digital Sky Survey. It implements integral field spectroscopy (IFU) to measure the spectra of hundreds of points in each galaxy, and its goal is to map the detailed composition and kinematic structure of 10,000 nearby galaxies [12]. MaNGA data cubes are available as FITS files on the Scientific Archive Server (SAS). We access the data using the Marvin package [12].

The data we used to model the J1436+4943 system is MaNGA's three-dimensional data cube. Its size is 4563 x 54 x 54. The first dimension represents the wavelength, and it has linear wavelength sampling from 3622.0 to 10353.0 Angstroms. The second and third dimensions are spatial dimensions in pixel, with a resolution of 0.5 arcsec per pixel. Figure 2 shows one example slice in this data cube, which corresponds to the wavelength 4559.319 Angstrom.

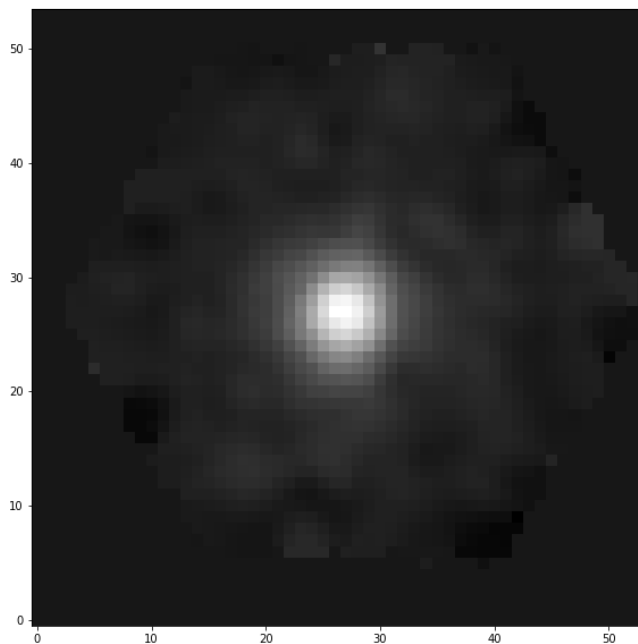


**Figure 2.** The image of one slice of the MaNGA's data cube, corresponding to the wavelength 4559.319 Angstroms. The image size is 54 x 54 in pixel with a resolution of 0.5 arcsec per pixel.

## 3. Emission Line Image Extraction

To accurately and efficiently analyze the lens system J1436+4943, it is crucial to do spectral feature extraction. The feature extraction includes two steps, feature conversion, and selection. The purpose is to extract information related to the target and eliminate other irrelevant information in the data as much as possible [13]. Strong lensing happens when the background source and the foreground lensing galaxy are well aligned. The alignment causes the images of the background source and the lensing galaxy to merge in the observed data. So, the first step is to perform foreground galaxy subtraction to extract the lensed emission-line image of the background source.

**Table 1.** The Emission Lines and their Restframe Wavelength. Column 2 presents the restframe vacuum wavelength of the emission lines.

Emission Line	Restframe Wavelength [Angstrom]
$O_{II}$	3727.09
$O_{II}$	3727.88

Previous studies revealed that the background [O<sub>II</sub>] emission of the system J1436+4943 has a redshift of 1.231, and apparently forms two separate arcs east and west of the target galaxy [1,10]. Therefore, we need to perform feature extraction to build the image of the [O<sub>II</sub>] band. The rest-frame wavelength of the O<sub>II</sub> emission line is 3727.09 Angstrom and 3729.88 Angstrom (listed in Table 1). Due to the cosmological redshift, which is determined by the distance between subjects, the observed wavelength of the O<sub>II</sub> emission line will differ from its rest frame wavelength. According to the following equation, the corresponding observed wavelength is 8317.37 Angstrom and 8323.60 Angstrom. Figure 3 shows one of the spectrums among the 54 x 54 pixels around the observed wavelength of the O<sub>II</sub> doublet emission line. There are two double peaks at corresponding wavelengths.

$$z = \frac{\lambda_{observed} - \lambda_{rest}}{\lambda_{rest}} \quad (1)$$

where  $z$  is the cosmological redshift,  $\lambda_{observed}$  is the observed wavelength,  $\lambda_{rest}$  is the emitted wavelength.

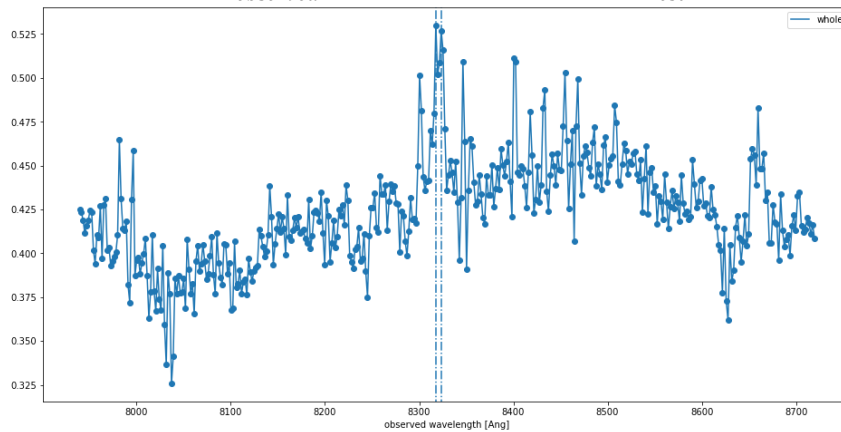


**Figure 3.** One of the spectrums in the data cube around the observed wavelength of the O<sub>II</sub> doublet emission line. The index of the spectrum among the 54 x 54 pixels are 26 and 23 for the second and third dimensions. The two vertical lines show the wavelengths of 8317.37 Angstrom and 8323.60 Angstrom.

For the next step, we used principal component analysis (PCA) to eliminate the continuum spectrum and extract the lensed images of the background source on the waveband of the O<sub>II</sub> doublet emission line. Principal component analysis decomposes and reorganizes many existing indicators to form a series of linearly independent comprehensive indicators, which can be sorted from high to low according to the ability to reflect the information contained in the original signal [13]. The purpose of data reduction and feature extraction can be achieved by only using a small number of comprehensive indicators with a strong descriptive ability for data analysis [13]. In this case, we can also take PCA as a way to detrend the spectrum.

First, we performed PCA on the data cube of the target system, and then reconstructed the approximated data cube with the first component from PCA, so that the final data only retains its main components, that is, the data of the foreground galaxy. The image of the lensed background source can be obtained by subtracting the continuum data from the original data. Figure 4 shows the net emission-line (O<sub>II</sub> doublet) image of the background source of system J1436+4943. Figure 5 is an example of the PCA result. The residual spectrum in figure 5 obtained by subtracting the continuum spectrum from the original spectrum is the spectrum of the lensed background source of the system J1436+4943.

#### 4. Modelling

Taking the net emission-line image after the PCA process, we reveal the physical properties of the lensing galaxy by lens modeling. We use Particle Swarm Optimization (PSO) [14] and Markov Chain Monte Carlo (MCMC) method in the modeling process, which are implemented in the Lenstronomy<sup>1</sup>. Lenstronomy is a multi-purpose software package that can be used for strong gravitational lens modeling [15]. It can be inferred from Figure 4 that this gravitational lens system has four lensed images, which is classical in strong lensing.

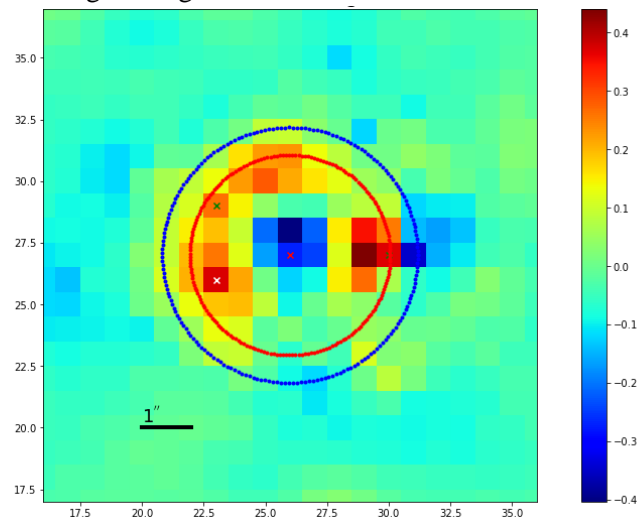


**Figure 4.** The net emission line ( $O_{II}$  doublet) image of the background source of system J1436+4943.  $\theta_{Ein} = 2.03$ (red) arcsec [1], and  $\theta_{Ein} = 2.59$  (blue) arcsec [10].

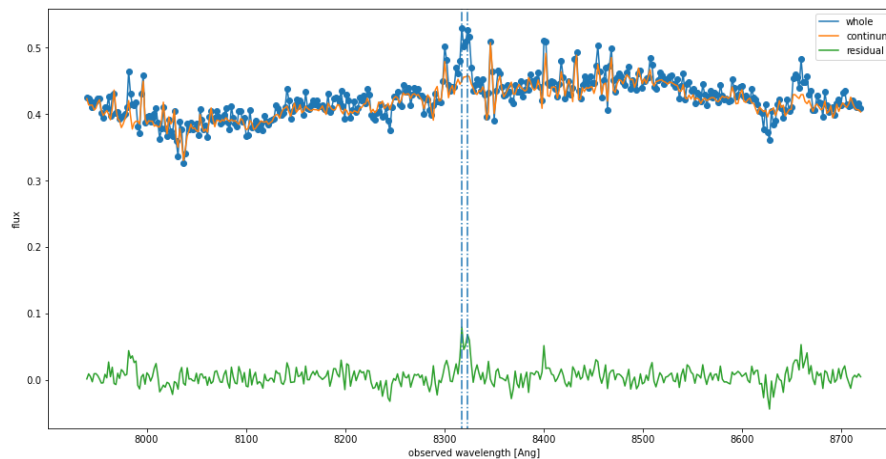


**Figure 5.** An example of the PCA result. The blue curve represents the original spectrum in the data. The orange curve is the reconstructed continuum spectrum with PCA. The green curve is the residual spectrum obtained by subtracting the continuum spectrum from the original spectrum. The  $O_{II}$  doublet emission line is clearly seen in the green curve. The pixel coordinates of these spectrums are (23, 26) in Figure 4 (marked with a white cross). The two vertical blue lines mark the wavelength of observed  $O_{II}$  doublet emission lines.

<sup>1</sup> <https://github.com/sibirrer/lenstronomy>

The singular isothermal ellipsoid (SIE) model is used to describe the lens surface mass distribution. The surface density profile  $\kappa(x, y)$  is defined as,

$$\kappa(x, y) = \frac{1}{2} \left( \frac{\theta_E}{\sqrt{qx^2 + y^2/q}} \right) \quad (2)$$

where  $\theta_E$  is the Einstein radius,  $q$  is the minor or major axis ratio, and  $x$  and  $y$  are defined in a coordinate system aligned with the major and minor axis of the lens.

We use the elliptical Sersic function to describe the source brightness distribution. The function used to return the Sersic profile value at  $(x, y)$  is,

$$I(R) = I_0 \exp \left[ -b_n (R/R_{Sersic})^{\frac{1}{n}} \right] \quad (3)$$

where  $I_0$  is the surface brightness value at the half-light radius,  $R = \sqrt{q\theta_x^2 + \theta_y^2/q}$ ,  $b_n \approx 1.999n - 0.327$ ,  $R_{Sersic}$  is the half-light radius,  $n$  is the Sersic index.

The relationship between the minor/major axis ratio,  $q$ , and the eccentricities,  $e_1$  and  $e_2$  is,

$$e_1 = (1 - q)/(1 + q) * \cos(2 * \phi) \quad (4)$$

$$e_2 = (1 - q)/(1 + q) * \sin(2 * \phi) \quad (5)$$

where  $e_1$  and  $e_2$  are the eccentricity parameter,  $q$  is the minor/major axis ratio,  $\phi$  is the angle of orientation (in radian).

To determine the optimal lensing parameters, we use the PSO algorithm first. The initial spread of parameters is set with hard upper and lower bound limits in parameter space. Then, the initial parameters and their limits are loaded into the PSO algorithm. As 14 parameters represent the MaNGA J1436+4943 system, the position vector of the PSO algorithm is a 14 dimensions vector. We use 150 particles to explore the parameter space to find the optimal parameter set. The process is iterated and converged in 80 steps. The local minimum found by the PSO algorithm is then taken as the initial parameter for the MCMC algorithm. In the left panel and the middle panel of Figure 6, there is an arc around the foreground galaxy observed and reconstructed from the input data. In the right panel of Figure 6, the residuals are dominated by random noise, so the PSO algorithm successfully finds the right model.

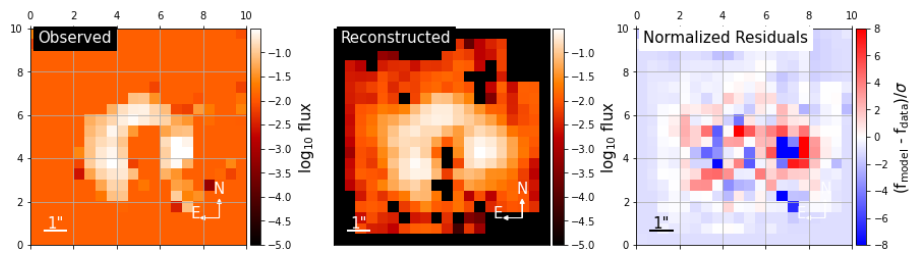


**Figure 6.** The left panel is the narrow-band emission-line image extracted from the MaNGA data cube. The middle panel is the reconstructed image from the PSO algorithm. The right panel is the normalized residuals between the model and the observed data. The net emission line ( $O_{II}$  doublet) image of the background source of system J1436+4943.  $\theta_{Ein} = 2.03$ (red) arcsec [1], and  $\theta_{Ein} = 2.59$  (blue) arcsec [10].

After the PSO algorithm, we use Markov chain Monte Carlo sampling to evaluate the uncertainties of model parameters. The MCMC algorithm, which appeared in the early 1950s, is a computer-simulated Monte Carlo method within Bayesian theory.

The result of the PSO algorithm is taken as the initial guess for the MCMC algorithm. Finally, the optimal parameter set is obtained. The  $\theta_E$  is 1.55 arcsec;  $e_1$  of the lens is -0.02,  $e_2$  of the lens is -0.02. The results of the PSO algorithm and MCMC algorithm are shown in the table below.

**Table 2.** Lens model parameters find by the PSO algorithm. Column 1 presents the model parameters of the lens. Column 2 shows the corresponding values.

Properties of the Lens	PSO results
$\theta_E$ (arcsec)	1.55
$e_1$	-0.025
$e_2$	-0.020

**Table 3.** Source model parameters find by the PSO algorithm. Column 1 presents the model parameters of the background sources. Column 2 shows the corresponding values.

Properties of the Background Sources	PSO results
$R_{Sersic}$	0.016
$n$	2.45
$e_1$	-0.056
$e_2$	0.49

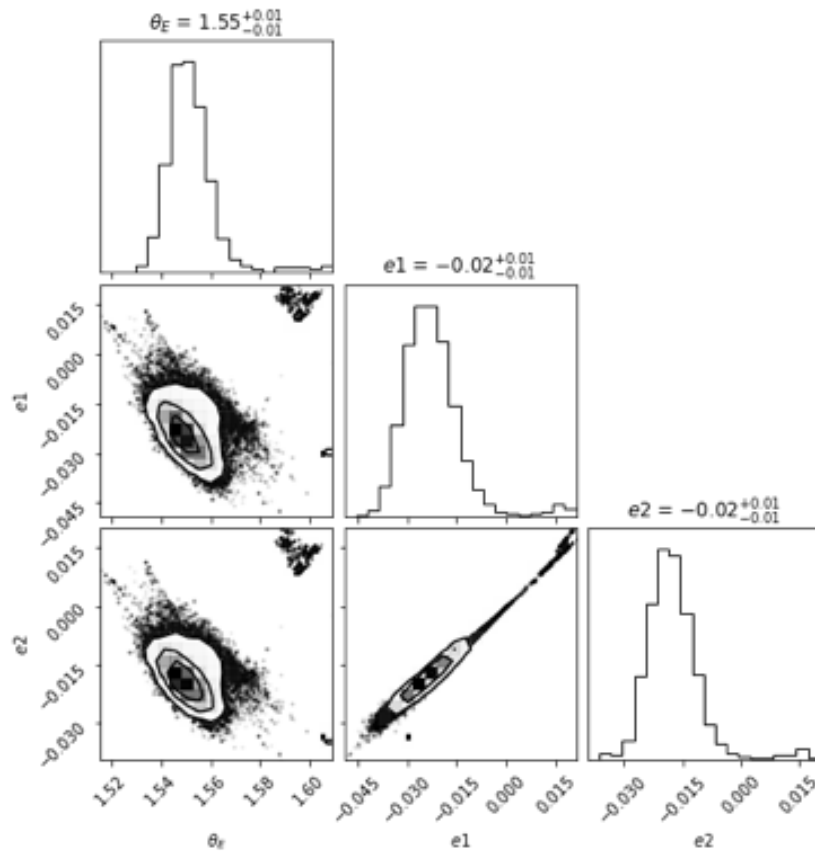


**Figure 7.** The corner plots of the samples from the MCMC algorithm.

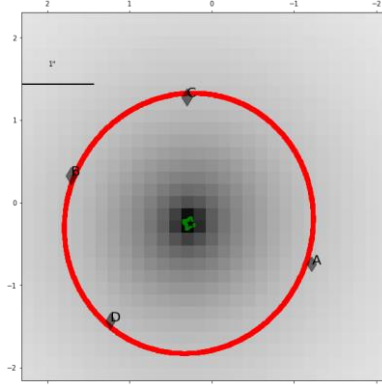


**Figure 8.** The relative positions of the four lensed images of the lens system J1436+4943 derived from the MCMC algorithm. The red curve represented the critical curve, the green curve is the caustics.

**Table 4.** Source model parameters find by the MCMC algorithm. Column 1 presents the model parameters of the background sources. Column 2 shows the corresponding values.

Properties of the Background Sources	MCMC results
$R_{Sersic}$	0.04
$n$	1.56
$e_1$	-0.05
$e_2$	0.49

**Table 5.** Lens model parameters find by the MCMC algorithm. Column 1 presents the model parameters of the lens. Column 2 shows the corresponding values.

Properties of the Lens	MCMC results
$\theta_E$ (arcsec)	$1.55^{+0.01}_{-0.01}$
$e_1$	-0.02
$e_2$	-0.02

## 5. Discussion

In this work, we test whether one can recover the properties of a strong lensing galaxy with only the MaNGA data. We compare the properties of the J1436+4943 system calculated using the MaNGA data in this paper with the properties of the J1436+4943 system derived from the FOCAS IFU data, so as to judge whether the data obtained by using only MaNGA data to study the strong gravitational lensing system is accurate and valid. The result shows that the general properties of the lens system can be found but the Einstein radius is different from the result with FOCAS IFU data by less than 25%. The  $\theta_E$  we derived is  $1.55 \pm 0.01$  arcsec, whereas the  $\theta_E$  derived from the FOCAS IFU data is  $2.03 \pm 0.04$  arcsec [1].

## 6. Conclusion

Although our results are not exactly the same as the results with FOCAS IFU data [1], the general properties of the lensing galaxy can still be obtained by using only the MaNGA data cube. Therefore, the MaNGA data cube can be used for strong gravitational lensing research. This will save the Subaru FOCAS IFU observation time since observing all the candidate lens systems found in the MaNGA survey data is expensive and time-consuming. Our results show that rapid analysis of a large sample in the MaNGA database is feasible, which benefits the investigation of the statistical properties of strong gravitational lensing systems.



## References

- [1] Smith, R. J. , Collier, W. P. , Shinobu, O. , & Lucey, J. R. . Subaru focus ifu observations of two  $z=0.12$  strong-lensing elliptical galaxies from sdss manga. *Monthly Notices of the Royal Astronomical Society: Letters*, 493 (1), L33-38 (2019).
- [2] Spingola, C., Mckean, J. P., Deller, A., & Moldon, J.. Gravitational lensing at milliarcsecond angular resolution with vlbi observations. In: the 14th European VLBI Network Symposium & Users Meeting, PoS(EVN2018)033. Sissa Medialab srl Partita, Granada, Spain (2019).
- [3] Ritondale, E., Vegetti, S., Despali, G., Auger, M. W., Koopmans, L., & Mckean, J. P.. Low-mass halo perturbations in strong gravitational lenses at redshift  $z \sim 0.5$  are consistent with  $\Lambda$ cdm. *Monthly Notices of the Royal Astronomical Society*, 485 (2), L2179-2193 (2019).
- [4] Hartley, P., (2019). "Finding and looking through strong gravitational lenses" [Ph.D. Thesis, The University of Manchester (United Kingdom)]. ProQuest Dissertations Publishing.
- [5] Browne, I., Wilkinson, P. N., Jackson, N., Myers, S. T., Fassnacht, C. D., & Koopmans, L., et al. The cosmic lens all-sky survey - ii. gravitational lens candidate selection and follow-up. *Monthly Notices of the Royal Astronomical Society*, 341 (1), L13-32 (2003).
- [6] Shepherd M.. Difmap: An Interactive Program for Synthesis Imaging. *Astronomical Data Analysis Software and Systems VI. ASP Conf. Ser. Vol. 125*, pp. 77-84 (1997).
- [7] Adam, S., Bolton, Scott, Burles, & Léon, et al. The sloan lens acs survey. i. a large spectroscopically selected sample of massive early-type lens galaxies\*. *The Astrophysical Journal*, 638 (2), L703-703 (2006).
- [8] Brownstein, J. R., Bolton, A. S., Schlegel, D. J., Eisenstein, D. J., Kochanek, C. S., & Connolly, N., et al. The boss emission-line lens survey (bells). i. a large spectroscopically selected sample of lens galaxies at redshift  $\sim 0.5$ . *Astrophysical Journal*, 744 (1), L41 (2012).
- [9] Hartley, P., Flamary, R., Jackson, N., Tagore, A. S., & Metcalf, R. B. Support vector machine classification of strong gravitational lenses. *Monthly Notices of the Royal Astronomical Society*, 471 (3), L3378-3397 (2017).
- [10] Talbot, M. S., Brownstein, J. R., Bolton, A. S., Kevin, B., Andrews, B. H., & Brian, C., et al. Sdss-iv manga: the spectroscopic discovery of strongly lensed galaxies. *Monthly Notices of the Royal Astronomical Society*, 477 (1), 195-209 (2018).
- [11] Ade, Peter AR, et al. Planck 2015 results-xiii. cosmological parameters. *Astronomy & Astrophysics* 594: A13 (2016).
- [12] Cherinka, B., Andrews, B. H., J Sánchez-Gallego, Brownstein, J., & Yan, R.. Marvin: a tool kit for streamlined access and visualization of the sdss-iv manga data set. *The Astronomical Journal*, 158 (2), L74 (2019).
- [13] LIXiang-ru. Feature Extracting Methods in Spectrum Data Mining. *Progress in Astronomy*, 30 (1), L94-105 (2012).
- [14] J. Kennedy and R. Eberhart, "Particle swarm optimization," *Proceedings of ICNN'95 International Conference on Neural Networks*, vol.4, pp. 1942-1948 (1995).
- [15] Birrer, S., Shajib, A., Gilman, D., Galan, A., & Amara, A.. Lenstronomy ii: a gravitational lensing software ecosystem. *The Journal of Open Source Software*, 6 (62), L3283-3291 (2021).